IL NUOVO CIMENTO **48 C** (2025) 57
DOI 10.1393/ncc/i2025-25057-6

Colloquia: IWM-EC 2024

Transient di-cluster systems: The Transient Rotational Model

A. Di Pietro(1) and A. C. Shotter(2)

(1) *INFN, Laboratori Nazionali del Sud - Catania, Italy*
(2) *School of Physics and Astronomy, University of Edinburgh - Edinburgh, UK*

received 26 November 2024

Summary. — Exotic clustering configurations are predicted to appear in the excited states of neutron-rich nuclei. These clusters are typically di-nuclear formations where one or both components consist of exotic neutron-rich nuclei. Here we discuss the results of ^{9}Li+^{4}He elastic scattering excitation function which shows very broad resonances at relatively high excitation energies that could be linked to this cluster formation. To better understand the nature of these broad resonances, the Transient Rotational Model has been developed. The main features of the model will be presented.

1. – Introduction

Exotic clustering configurations consist of di-nuclear systems, where one or both clusters are composed of neutron-rich nuclei [1]. They are expected to emerge in the excited states of neutron-rich nuclei. A way to experimentally observe them is by measuring the elastic scattering excitation function involving neutron-rich nuclei. The scattering, in fact, might be influenced by the rotational band structure of the compound nucleus; resonances in the elastic scattering excitation function, however, could be due to effects other than compound nucleus formation having dynamic origin instead, originated by the extended surface of neutron-rich nuclei [2-11].

Broad resonances in the elastic scattering excitation function at relatively high excitation energies are observed in the reaction ^{9}Li + ^{4}He. Those resonances have backward-peaked angular distributions associated with high angular momentum. To describe these resonances a possible scenario involves the ^{4}He being temporarily captured by the weak attraction of the neutron tail of the neutron-rich ^{9}Li, causing the two nuclei to orbit each other. This transient state may lead to the re-emission of ^{4}He into the entrance channel, as a result, broad resonances may appear in the elastic excitation function. To explain the origin of these broad resonances, a simple model, called the Transient Rotational Model (TRM), was developed. In this paper the basic concepts of the model are highlighted.

Creative Commons Attribution 4.0 License (https://creativecommons.org/licenses/by/4.0)

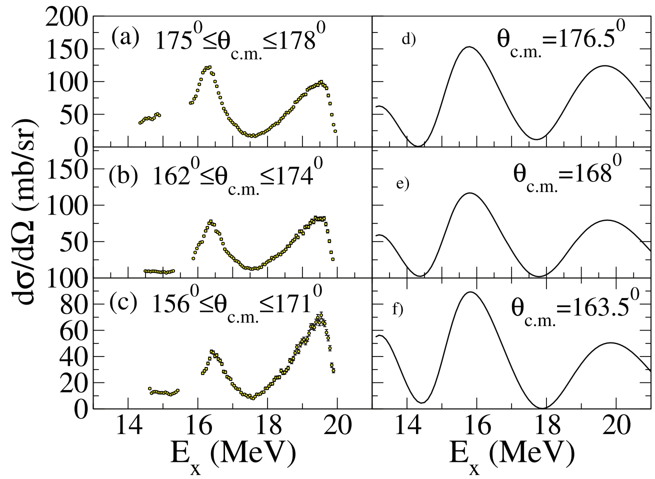

Fig. 1. – Left: experimental differential cross-section for the reaction ^{4}He(^{9}Li, ^{9}Li) ^{4}He as a function of E_x. Panel (a) corresponds to data collected in the c.m. angular range $175° \le \theta_{c.m} \le 178°$, (b) $162° \le \theta_{c.m} \le 174°$, (c) $156° \le \theta_{c.m} \le 171°$. Right: TRM calculations at the corresponding mean c.m. angles of (d) 176.5°, (e) 168°, and (f) 163.5°.

2. – Experiment

The ^{9}Li + ^{4}He experiment was conducted at TRIUMF in Canada using a 32 MeV ^{9}Li beam which was directed at a ^{4}He gas target. The Thick Target Inverse Kinematic (TTIK) technique was used. The ^{9}Li beam was stopped in the gas before reaching the detectors placed at 0° in the laboratory. The recoiling alpha particles, having lower stopping power than the beam, were detected. The target was made of ^{4}He gas at 650 Torr. A 12 μm-thick Kapton window was used to separate the gas-filled chamber from the high-vacuum beam line. Elastically scattered α-particles were detected and distinguished from other reaction processes using Time of Flight (ToF) techniques. For an extended target, ToF measurements allow for the discrimination of elastic scattering from other events, such as inelastic scattering. To measure ToF, a microchannel plate (MCP) detector was placed upstream of the Kapton window under vacuum, generating a signal each time a ^{9}Li particle entered the chamber. It was also used for cross-section normalization. The detection system comprised three telescopes, each consisting of a $50 \times 50\,\text{mm}^2$, 50 μm-thick silicon detector segmented into four quadrants as ΔE, and a $50 \times 50\,\text{mm}^2$, 1500 μm-thick single PAD silicon detector for residual energy detection.

The compound nucleus ^{13}B excitation function was obtained from the center-of-mass energy spectrum by adding the two-body $Q_{val} = 10.82$ MeV. Figure 1 displays the excitation functions at the three angular c.m. ranges, $175° \le \theta_{c.m} \le 178°$, $162° \le \theta_{c.m} \le 174°$ and $156° \le \theta_{c.m} \le 171°$ covered by the detectors. The cross-section in fig. 1 reveals broad peaks having an angular distribution, shown in fig. 2, that is most prominent at backward angles.

3. – The TRM model

Broad resonances in the compound nucleus at high excitation energy may suggests the presence of molecular-type resonances. The way a nuclear reaction is influenced by the

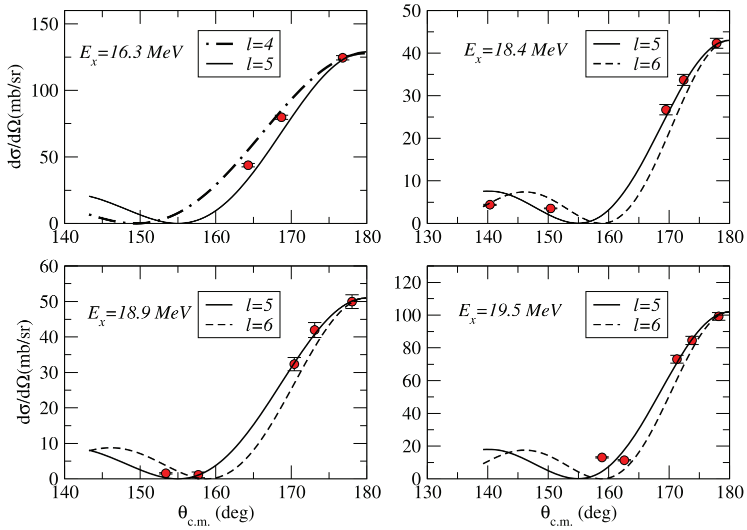

Fig. 2. – Symbols: angular distribution at four excitation energies. $\ell = 4$ (dot-dashed line), $\ell = 5$ (full line), $\ell = 6$ (dashed line) Legendre polynomials normalised to the experimental cross-section at the most backward c.m. angle.

surface region of the colliding nuclei has been of interest for many years [2-11]. Beyond the Coulomb barrier, shape resonances can appear at angular momentum $\ell \sim$ kR, corresponding to quasi-molecular states with angular distributions characteristic of ℓ. The reaction process can be described as projectile and target touching at their surfaces, *i.e.*, at an impact parameter close to the sum of their radii; the two nuclei then separate after a rolling motion. A model called the Transient Rotational Model was developed in [12], and described in detail in [13], to explain this phenomenon. The scattering of a weakly bound neutron-rich nucleus ^{9}Li on ^{4}He is described by a double Woods-Saxon (W-S) potential rather than a single potential, one corresponding to the scattering from the core and the other corresponding to the scattering from the surface [13]. The parameters of the model for the reaction ^{4}He(^{9}Li, ^{9}Li) were derived from the work of Kanada En'yo *et al.* [1]. The W-S potential diffuseness, both for the core and the surface, was considered to be zero. With the chosen potential parameters, the calculated elastic scattering excitation function ^{4}He(^{9}Li, ^{9}Li) predicts the presence of two resonances closely matching the energies and cross-section magnitudes of the experimental 16.4 and 19.5 MeV resonances observed in the ^{9}Li + ^{4}He study. The probability amplitude $P(r, \theta, \phi) = |\Psi(r, \theta, \phi)|^2$, and the probability flux $F(r, \theta, \phi) = \frac{i\hbar}{2\mu}(\Psi \nabla \Psi^* - \Psi^* \nabla \Psi)$, have been calculated for the resonance energy $E_x = 19.5$ MeV. $\Psi(r, \theta, \phi)$ is the total wave function [13]. Figure 3 presents the TRM results for these two quantities based on the double W-S potential described above. Figures 3(a) and (b) show the TRM results when the calculation includes both Coulomb and nuclear core and surface potentials. The surface is located between the two red circles. While upstream standing waves still occur due to the reflection of the incoming wave, part of the incoming wave becomes trapped within the surface and begins to rotate around it. Additionally, there seems to be a standing wave, likely resulting from constructive interference between fluxes on opposite sides of the shell. As shown in fig. 2 the resonance at $E_x = 19.5$ MeV is consistent with an angular momentum

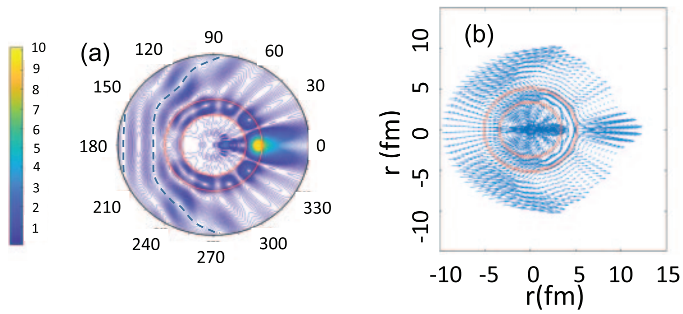

Fig. 3. – TRM probability intensity (a), $P(r, \theta, \phi)$, and probability flux (b), $F(r, \theta, \phi)$, calculated for the ^{9}Li(^{4}He, ^{4}He)^{9}Li, corresponding to $E_x = 19.5$ MeV. The inner red circle radius ($r_c = 3.4$ fm) corresponds to the core potential radius, and outer circle radius ($r_s = 5.1$ fm) corresponds to the surface radius. $P(r, \theta, \phi)$ is plotted as contours of equal intensity at (r, θ) points. The beam is going from left to right. $F(r, \theta, \phi)$ is represented by vectors at (r, θ) points whose length corresponds to the flux magnitude along the vector direction.

quantum number $\ell = 5$. This is in agreement with the number of peaks or nodes around the surface of $P(r, \theta, \phi)$ as shown in fig. 3(a). In fig. 3 it can also be seen that part of the incoming flux is absorbed into the core and some is also being pulled back from the core and ejected forward.

Using the TRM model the elastic scattering angular distributions ^{9}Be + ^{4}He in the energy range 10 MeV $\leq E_{c.m.} \leq$ 20 MeV reported in [14] are also analysed. The results of the TRM fit are shown in fig. 4. As can be seen in the Figure, the TRM model reproduces very well the data with the choice of the potential parameters reported in [13]. This gives some confidence concerning the value of the TRM approach to interpret reactions of this type.

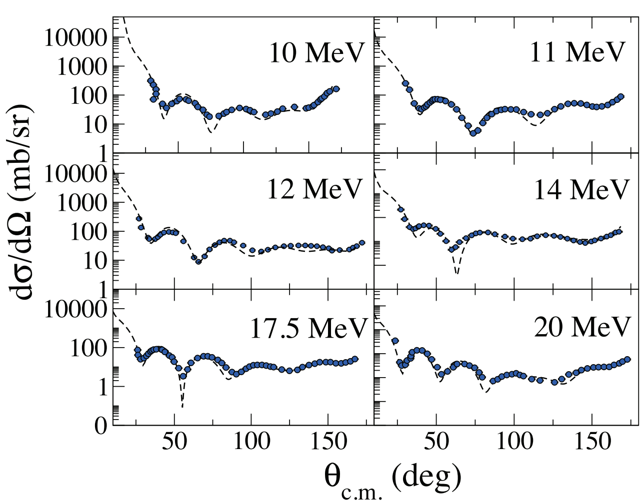

Fig. 4. – Symbols: ^{9}Be(^{4}He, ^{4}He)^{9}Be reaction at six laboratory energies from 10 to 20 MeV from [14]. Dashed lines are best TRM fits to the data.

4. – Summary

The excitation function for the reaction $^{9}\mathrm{Li} + {}^{4}\mathrm{He}$ shows broad resonances at high excitation energies with angular distributions indicating high angular momentum. To explain these resonances, the Transient Rotational Model was developed. Within this model, these broad resonances result from a transient state in which ^{4}He is weakly captured by the neutron-rich tail of ^{9}Li, causing the nuclei to orbit each other before re-emission. This simple model accurately predicts two resonances with energies and cross-sections in agreement with the observed resonances at $E_x = 16.4$ and $19.5\,\mathrm{MeV}$. The TRM wave function derived form the analysis of the $^{9}\mathrm{Li}+{}^{4}\mathrm{He}$ scattering data, for the resonance at $E_x = 19.5\,\mathrm{MeV}$, clearly shows evidence of a resonance structure within the surface region. These surface resonances can be as large and as relevant in enhancing the elastic cross-section as the compound nucleus ones which are due to absorption from the core.

REFERENCES

[1] Kanada-En'yo Y., Kawanami Y., Taniguchi Y. and Kimura M., *Theor. Phys.*, **120** (2008) 917.
[2] Braun-Munzinger P. and Barrette J., *Phys. Rep.*, **87** (1982) 209.
[3] Bosanac S., *Phys. Rev. A*, **19** (1979) 125.
[4] Landowne S., *Phys. Rev. Lett.*, **42** (1979) 633.
[5] Fuller R., *Nucl. Phys. A*, **216** (1973) 199.
[6] Tamura T. and Wolter H., *Phys. Rev. C*, **6** (1972) 1976.
[7] Arima A., Scharff-Goldhaber G. and McVoy K., *Phys. Lett. B*, **40** (1972) 7.
[8] McVoy K., *Phys. Rev. C*, **3** (1971) 1104.
[9] Sokolovski D., Msezane A., Felfli Z., Ovchinnikov S. and Macek J. H., *Nucl. Instrum. Methods B*, **261** (2007) 133.
[10] Friedman W. and McVoy K., *Phys. Lett. B*, **87** (1979) 179.
[11] Cowley A. and Heymann G., *Nucl. Phys. A*, **146** (1970) 465.
[12] Di Pietro, Alessia *et al.*, *Phys. Lett. B*, **832** (2022) 137256.
[13] Shotter Alan C. and Di Pietro Alessia, *Phys. Rev. C*, **110** (2024) 034603.
[14] Taylor R., Fletcher N. and Davis R., *Nucl. Phys.*, **65** (1965) 318.